Efficient Time Integration Strategies for High Order Discontinuous Galerkin Time Domain Methods

A. Catella[1] V. Dolean[1,2] L. Fezoui[1] S. Lanteri[1]

[2]University of Nice-Sophia Antipolis
J.A. Dieudonné Mathematics Laboratory, UMR CNRS 6621, 06108 Nice Cedex, France
[1]INRIA, NACHOS project-team
2004 Route des Lucioles, BP 93, 06902 Sophia Antipolis Cedex, France

ACES Conference
The Annual Review of Progress in Applied Computational Electromagnetics
March 30 - April 4, 2008, Niagara Falls, Canada

Content

Outline

Context and motivations

- Time-domain electromagnetic wave propagation
- Irregularly shaped geometries
  - Unstructured, locally refined, triangular (2D)/tetrahedral (3D) meshes
- Numerical ingredients (starting point of this study)
  - Discontinuous Galerkin time-domain (DGTD) methods
  - Nodal (Lagrange type) polynomial interpolation
  - Explicit time integration

Context and motivations

- Scattering of a plane wave by an aircraft, F=1 GHz
  - Mesh: # vertices = 153,821 , # tetrahedra = 883,374
  - $L_{\mathrm{min}} = 0.000601$ m , $L_{\mathrm{max}} = 0.121290$ m $(\approx \dfrac{\lambda}{2.5})$, $L_{\mathrm{avg}} = 0.039892$ m
  - $\Delta t_{\mathrm{min}} =$ 0.24 picosec and $\Delta t_{\mathrm{max}} = 40.50$ picosec

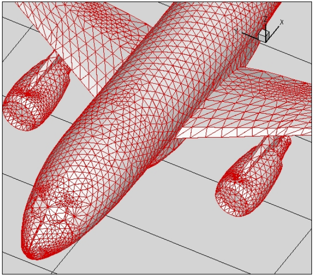

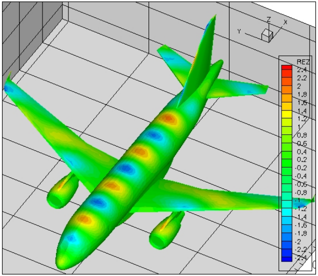

Context and motivations

- Possible routes to overcome grid-induced stiffness
  - Local time-step strategies with explicit time integration
  - Locally implicit (hybrid explicit/implicit) time integration

- Overall objectives of this study
  - Investigate strengthes and weaknesses of implicit and hybrid explicit/implicit DGTD methods
  - Theoretical and numerical aspects (stability, convergence, etc.)
  - Computational aspects
    - Linear system solvers
    - Parallel computing

Context and motivations

Implicit and hybrid explicit/implicit time-domain methods

- Several works on ADI-FDTD
  - T. Namiki, IEEE Trans. Microwave Theory Tech., 2000
  - F. Zheng and Z. Chen, IEEE Trans. Microwave Theory Tech., 2001
    - Numerical dispersion analysis
  - S.G. Garcia and T.W. Lee and S.C. Hagness
    IEEE Trans. Antennas and Wir. Propag. Lett., 2002
    - Accuracy analysis
- Hybrid explicit/implicit method
  - Explicit FDTD + Implicit FETD (triangular meshes)
  - T.R. Rylander, A. Bondeson, Comput. Phys. Commun., 2000
  - T.R. Rylander, A. Bondeson, J. Comput. Phys. 2002
  - T. Halleröd, T.R. Rylander, J. Comput. Phys. 2008
- Implicit DGTD method in 2D
  - A. Catella, V. Dolean and S. Lanteri
    IEEE. Trans. Magn., to appear. Also INRIA RR-6110, 2007

Outline

DG-$\mathbb{P}_p$ method for Maxwell equations

- Time-domain Maxwell's equations

$$\varepsilon \partial_t \mathbf{E} - \nabla \times \mathbf{H} = 0 \quad \text{and} \quad \mu \partial_t \mathbf{H} + \nabla \times \mathbf{E} = 0$$

- Boundary conditions: $\partial\Omega = \Gamma_a \cup \Gamma_m$

$$\begin{cases} \mathbf{n} \times \mathbf{E} = 0 \text{ on } \Gamma_m \\ \mathbf{n} \times \mathbf{E} - \sqrt{\dfrac{\mu}{\varepsilon}} \mathbf{n} \times (\mathbf{H} \times \mathbf{n}) = \mathbf{n} \times \mathbf{E}_{\text{inc}} - \sqrt{\dfrac{\mu}{\varepsilon}} \mathbf{n} \times (\mathbf{H}_{\text{inc}} \times \mathbf{n}) \text{ on } \Gamma_a \end{cases}$$

- Triangulation of Ω: $\overline{\Omega_h} \equiv \mathcal{T}_h = \bigcup_{\tau_i \in \mathcal{T}_h} \overline{\tau}_i$
  - Approximation space: $V_h = \{\mathbf{V}_h \in L^2(\Omega)^3 \mid \forall i, \mathbf{V}_{h|\tau_i} \equiv \mathbf{V}_i \in \mathbb{P}_p(\tau_i)^3\}$
  - Variational formulation: $\forall \vec{\varphi} \in \mathcal{P}_i = \text{Span}(\vec{\varphi}_{ij} \ , \ 1 \leq j \leq d_i)$

$$\begin{cases} \displaystyle\iiint_{\tau_i} \vec{\varphi} \cdot \varepsilon_i \partial_t \mathbf{E} d\omega = -\iint_{\partial\tau_i} \vec{\varphi} \cdot (\mathbf{H} \times \vec{n}) d\sigma + \iiint_{\tau_i} \nabla \times \vec{\varphi} \cdot \mathbf{H} d\omega \\ \displaystyle\iiint_{\tau_i} \vec{\varphi} \cdot \mu_i \partial_t \mathbf{H} d\omega = \iint_{\partial\tau_i} \vec{\varphi} \cdot (\mathbf{E} \times \vec{n}) d\sigma - \iiint_{\tau_i} \nabla \times \vec{\varphi} \cdot \mathbf{E} d\omega \end{cases}$$

- Approximate fields: $\forall i$, $\mathbf{E}_{h|\tau_i} \equiv \mathbf{E}_i$ and $\mathbf{H}_{h|\tau_i} \equiv \mathbf{H}_i$
- Integral over $\partial\tau_i$: $\mathbf{E}_{|_{a_{ik}}} = \dfrac{\mathbf{E}_i + \mathbf{E}_k}{2}$ and $\mathbf{H}_{|_{a_{ik}}} = \dfrac{\mathbf{H}_i + \mathbf{H}_k}{2}$
- Assume $\Gamma_a = \emptyset$ (for the presentation only) and on Γ_m: $\mathbf{E}_{k|_{a_{ik}}} = -\mathbf{E}_{i|_{a_{ik}}}$ and $\mathbf{H}_{k|_{a_{ik}}} = \mathbf{H}_{i|_{a_{ik}}}$

$$
\left\{
\begin{aligned}
\iiint\limits_{\tau_i} \vec{\varphi} \cdot \varepsilon_i \partial_t \mathbf{E}_i d\omega &= \frac{1}{2} \iiint\limits_{\tau_i} (\nabla \times \vec{\varphi} \cdot \mathbf{H}_i + \nabla \times \mathbf{H}_i \cdot \vec{\varphi}) d\omega \\
&- \frac{1}{2} \sum_{k \in \mathcal{V}_i} \iint\limits_{a_{ik}} \vec{\varphi} \cdot (\mathbf{H}_k \times \vec{n}_{ik}) d\sigma \\
\iiint\limits_{\tau_i} \vec{\varphi} \cdot \mu_i \partial_t \mathbf{H}_i d\omega &= -\frac{1}{2} \iiint\limits_{\tau_i} (\nabla \times \vec{\varphi} \cdot \mathbf{E}_i + \nabla \times \mathbf{E}_i \cdot \vec{\varphi}) d\omega \\
&+ \frac{1}{2} \sum_{k \in \mathcal{V}_i} \iint\limits_{a_{ik}} \vec{\varphi} \cdot (\mathbf{E}_k \times \vec{n}_{ik}) d\sigma
\end{aligned}
\right.
$$

- Local projections

$$\mathbf{E}_i(\mathbf{x}) = \sum_{1\leq j\leq d_i} E_{ij}\vec{\varphi}_{ij}(\mathbf{x}) \text{ and } \mathbf{H}_i(\mathbf{x}) = \sum_{1\leq j\leq d_i} H_{ij}\vec{\varphi}_{ij}(\mathbf{x})$$

- Vector representation of local fields

$$\mathbb{E}_i = \{E_{ij}\}_{1\leq j\leq d_i} \textit{ and } \mathbb{H}_i = \{H_{ij}\}_{1\leq j\leq d_i}$$

- For $1 \leq j, l \leq d_i$:
    - $(\mathbf{M}_i^{\varepsilon})_{jl} = \varepsilon_i \iiint\limits_{\tau_i} {}^{\mathrm{T}}\vec{\varphi}_{ij}\vec{\varphi}_{jl} d\omega$ and $(\mathbf{M}_i^{\mu})_{jl} = \mu_i \iiint\limits_{\tau_i} {}^{\mathrm{T}}\vec{\varphi}_{ij}\vec{\varphi}_{jl} d\omega$
    - $(\mathbf{K}_i)_{jl} = \dfrac{1}{2} \iiint\limits_{\tau_i} ({}^{\mathrm{T}}\vec{\varphi}_{ij}\nabla \times \vec{\varphi}_{il} + {}^{\mathrm{T}}\vec{\varphi}_{il}\nabla \times \vec{\varphi}_{ij}) d\omega$

- For $1 \leq j \leq d_i$ and $1 \leq l \leq d_k$
    - $(\mathbf{S}_{ik})_{jl} = \dfrac{1}{2} \iint\limits_{a_{ik}} {}^{\mathrm{T}}\vec{\varphi}_{ij}(\vec{\varphi}_{kl} \times \vec{n}_{ij}) d\sigma$

- Local EDO systems

$$\forall \tau_i \quad : \quad \begin{cases} \mathbf{M}_i^{\varepsilon} \dfrac{d\mathbb{E}_i}{dt} = \mathbf{K}_i \mathbb{H}_i - \displaystyle\sum_{k \in \mathcal{V}_i} \mathbf{S}_{ik} \mathbb{H}_k \\ \mathbf{M}_i^{\mu} \dfrac{d\mathbb{H}_i}{dt} = -\mathbf{K}_i \mathbb{E}_i + \displaystyle\sum_{k \in \mathcal{V}_i} \mathbf{S}_{ik} \mathbb{E}_k \end{cases}$$

- Global EDO systems with $d = \sum_i d_i$

$$\mathbf{M}^{\varepsilon} \frac{d\mathbb{E}}{dt} = \mathbf{F}\mathbb{H} \quad \text{and} \quad \mathbf{M}^{\mu} \frac{d\mathbb{H}}{dt} = -{}^{\mathsf{T}}\mathbf{F}\mathbb{E}$$

  - $\mathbf{F} = \mathbf{K} - \mathbf{A} - \mathbf{B}$
  - $\mathbf{M}^{\varepsilon}$ are $\mathbf{M}^{\mu}$ block diagonal symmetric definite positive matrices
  - $\mathbf{K}$ is a $d \times d$ block diagonal symmetric matrix
  - $\mathbf{A}$ is a $d \times d$ block sparse symmetric matrix (internal faces)
  - $\mathbf{B}$ is a $d \times d$ block sparse skew symmetric matrix (metallic faces)

Outline

Explicit DGTD-$\mathbb{P}_p$ method

- L. Fezoui, S. Lanteri, S. Lohrengel and S. Piperno
  ESAIM: M2AN, Vol. 39, No. 6, 2005
  - Tetrahedral meshes, high order Lagrange polynomials
  - Leap-Frog time integration scheme, centered fluxes

$$\left\{ \begin{array}{lcl} \mathbf{M}^{\varepsilon} \dfrac{\mathbb{E}^{n+1} - \mathbb{E}^{n}}{\Delta t} & = & \mathbf{F}\mathbb{H}^{n+\frac{1}{2}} \\ \mathbf{M}^{\mu} \dfrac{\mathbb{H}^{n+\frac{1}{2}} - \mathbb{H}^{n-\frac{1}{2}}}{\Delta t} & = & -{}^{\mathsf{T}}\mathbf{F}\mathbb{E}^{n+1} \end{array} \right.$$

Outline

Implicit DGTD-$\mathbb{P}_p$ method

- A. Catella, V. Dolean and S. Lanteri
  IEEE. Trans. Magn., to appear. Also INRIA RR-6110, 2007
  - Triangular meshes, high order Lagrange polynomials
  - Crank-Nicolson time integration scheme, centered fluxes

$$\begin{cases} \mathbf{M}^{\varepsilon} \dfrac{\mathbb{E}^{n+1} - \mathbb{E}^{n}}{\Delta t} = \mathbf{F} \dfrac{\mathbb{H}^{n+1} + \mathbb{H}^{n}}{2} \\ \mathbf{M}^{\mu} \dfrac{\mathbb{H}^{n+1} - \mathbb{H}^{n}}{\Delta t} = -{}^{\mathsf{T}}\mathbf{F} \dfrac{\mathbb{E}^{n+1} + \mathbb{E}^{n}}{2} \end{cases}$$

  - Properties of the fully discrete scheme
    - Unconditional stability
      $\mathcal{E}_h^n = {}^{\mathsf{T}}\mathbb{E}^n \mathbf{M}^{\varepsilon} \mathbb{E}^n + {}^{\mathsf{T}}\mathbb{H}^n \mathbf{M}^{\mu} \mathbb{H}^n$ is exactly conserved (when $\Gamma_a = \emptyset$)
    - Convergence: deduced from the study for the explicit DGTD-$\mathbb{P}_p$ method
      $$\mathcal{O}(Th^{\min(s,p)}) + \mathcal{O}(\Delta t^2)$$
    - Invertibility of the associated linear system

- Two-dimensional Maxwell's equation (TM)

$$\begin{cases} \mu \dfrac{\partial H_x}{\partial t} + \dfrac{\partial E_z}{\partial y} = 0 \\ \mu \dfrac{\partial H_y}{\partial t} - \dfrac{\partial E_z}{\partial x} = 0 \\ \varepsilon \dfrac{\partial E_z}{\partial t} - \dfrac{\partial H_y}{\partial x} + \dfrac{\partial H_x}{\partial y} = 0 \end{cases}$$

- Implicit DGTD-$\mathbb{P}_p$ method
    - Triangular mesh
    - Sparse block matrix, $3n_p \times 3n_p$ (with $n_p = ((p+1)(p+2))/2$)
    - MUMPS multifrontal sparse matrix solver
      (P.R. Amestoy, I.S. Duff and J.-Y. L'Excellent, CMAME, Vol. 184, 2000)
    - LU factors computed before entering the time stepping loop

Numerical results
Eigenmode in a metallic cavity

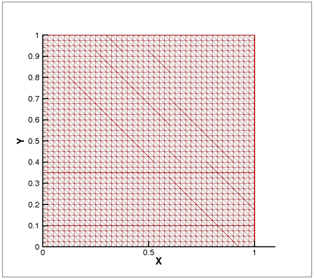

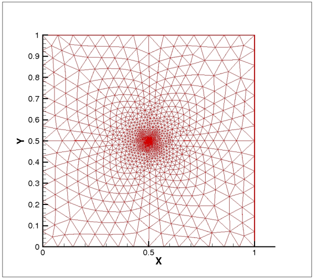

\# vertices = 1,681
\# elements = 3,200

$(\Delta t)_u = 58.92$ picosec

\# vertices = 1,400
\# elements = 2,742

$(\Delta t)_m = 1.44$ picosec
$(\Delta t)_M = 235.54$ picosec

Numerical results
Eigenmode in a metallic cavity

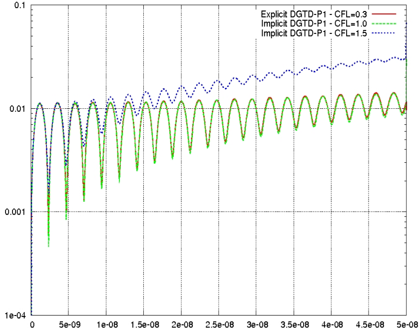

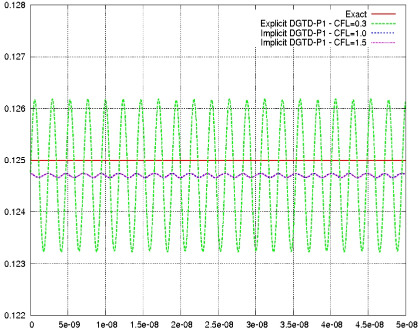

DGTD-$\mathbb{P}_1$ method: time evolutions of the L2 error (left) and discrete energy (right)
Uniform mesh

Numerical results
Eigenmode in a metallic cavity

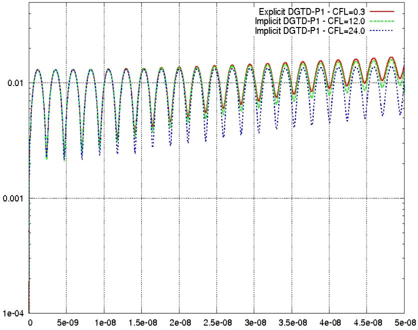

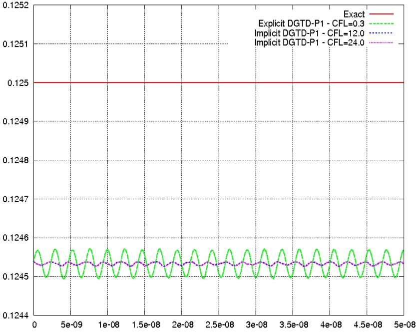

DGTD-$\mathbb{P}_1$ method: time evolutions of the L2 error (left) and discrete energy (right)
Non-uniform mesh

Numerical results
Eigenmode in a metallic cavity

Computing times (AMD Opteron 2 GHz based workstation)

Time integration	Method	CFL-$\mathbb{P}_p$	CPU time
Explicit	DGTD-$\mathbb{P}_1$	0.3	15 sec
Implicit	-	1.0	44 sec
-	-	1.5	30 sec

Uniform mesh

Time integration	Method	CFL-$\mathbb{P}_p$	CPU time
Explicit	DGTD-$\mathbb{P}_1$	0.3	443 sec
Implicit	-	12.0	133 sec
-	-	24.0	67 sec
Explicit	DGTD-$\mathbb{P}_2$	0.2	2057 sec
Implicit	-	2.0	1923 sec
-	-	4.0	938 sec
-	-	6.0	620 sec

Non-uniform mesh

Factorization: CPU time, RAM size (LU/total)
$<$ 1 sec, 13 MB/26 MB (DGTD-$\mathbb{P}_1$) and 2 sec, 34 MB/64 MB (DGTD-$\mathbb{P}_2$)

Outline

Hybrid explicit/implicit DGTD-$\mathbb{P}_p$ method

- S. Piperno, ESAIM: M2AN, Vol. 40, No. 5, 2006
  - Explict scheme: Verlet method (i.e. three-step Leap-Frog method with **E** and **H** computed at the same time stations)
  - Implicit scheme: Crank-Nicolson scheme
- Partitioning of the mesh elements (triangles/tetrahedra) into two subsets
  - $\mathcal{S}^e$: coarsest elements, treated explicitly
  - $\mathcal{S}^i$: smallest elements, treated implicitly

$$\mathbb{E} = \begin{pmatrix} \mathbb{E}_e \\ \mathbb{E}_i \end{pmatrix} \quad , \quad \mathbb{H} = \begin{pmatrix} \mathbb{H}_e \\ \mathbb{H}_i \end{pmatrix}$$

$$\mathbf{M}^\varepsilon = \begin{pmatrix} \mathbf{M}_e^\varepsilon & \mathbf{O} \\ \mathbf{O} & \mathbf{M}_i^\varepsilon \end{pmatrix} \; , \; \mathbf{M}^\mu = \begin{pmatrix} \mathbf{M}_e^\mu & \mathbf{O} \\ \mathbf{O} & \mathbf{M}_i^\mu \end{pmatrix}$$

$$\mathbf{K} = \begin{pmatrix} \mathbf{K}_e & \mathbf{O} \\ \mathbf{O} & \mathbf{K}_i \end{pmatrix} \; , \; \mathbf{B} = \begin{pmatrix} \mathbf{B}_e & \mathbf{O} \\ \mathbf{O} & \mathbf{B}_i \end{pmatrix}$$

Hybrid explicit/implicit DGTD-$\mathbb{P}_p$ method

- $\mathbf{A}$: matrix corresponding to fluxes at cell interfaces
  - $\mathbf{A}_{ee}$ and $\mathbf{A}_{ii}$ are symmetric matrices
  - $\mathbf{A}_{ei} = {}^{\mathsf{T}}\mathbf{A}_{ie}$

$$\mathbf{A} = \begin{pmatrix} \mathbf{A}_{ee} & \mathbf{A}_{ei} \\ \mathbf{A}_{ie} & \mathbf{A}_{ii} \end{pmatrix}$$

- $\mathbf{G}_e = \mathbf{K}_e - \mathbf{A}_{ee} + \mathbf{B}_e$
- $\mathbf{G}_i = \mathbf{K}_i - \mathbf{A}_{ii} + \mathbf{B}_i$
- $\mathbf{G}_e$ and $\mathbf{G}_i$ are symmetric matrices

$$\left\{ \begin{array}{rcl} \mathbf{M}^{\varepsilon} \dfrac{d\mathbb{E}}{dt} & = & \mathbf{F}\mathbb{H} \\ \mathbf{M}^{\mu} \dfrac{d\mathbb{H}}{dt} & = & -{}^{\mathsf{T}}\mathbf{F}\mathbb{E} \end{array} \right. \iff \begin{array}{l} \left\{ \begin{array}{rcl} \mathbf{M}^{\varepsilon}_e \dfrac{d\mathbb{E}_e}{dt} & = & \mathbf{G}_e\mathbb{H}_e - \mathbf{A}_{ei}\mathbb{H}_i \\ \mathbf{M}^{\mu}_e \dfrac{d\mathbb{H}_e}{dt} & = & -{}^{\mathsf{T}}\mathbf{G}_e\mathbb{E}_e + \mathbf{A}_{ei}\mathbb{E}_i \end{array} \right. \\ \left\{ \begin{array}{rcl} \mathbf{M}^{\varepsilon}_i \dfrac{d\mathbb{E}_i}{dt} & = & \mathbf{G}_i\mathbb{H}_i - \mathbf{A}_{ie}\mathbb{H}_e \\ \mathbf{M}^{\mu}_i \dfrac{d\mathbb{H}_i}{dt} & = & -{}^{\mathsf{T}}\mathbf{G}_i\mathbb{E}_i + \mathbf{A}_{ie}\mathbb{E}_e \end{array} \right. \end{array}$$

Hybrid explicit/implicit DGTD-$\mathbb{P}_p$ method

$$\left\{\begin{array}{lcl}
\mathbf{M}_e^{\mu}\dfrac{\mathbb{H}_e^{n+\frac{1}{2}}-\mathbb{H}_e^{n}}{\Delta t/2} & = & -{}^{\mathsf{T}}\mathbf{G}_e\mathbb{E}_e^{n}+\mathbf{A}_{ei}\mathbb{E}_i^{n} \\[2ex]
\mathbf{M}_e^{\varepsilon}\dfrac{\mathbb{E}_e^{n+\frac{1}{2}}-\mathbb{E}_e^{n}}{\Delta t/2} & = & \mathbf{G}_e\mathbb{H}_e^{n+\frac{1}{2}}-\mathbf{A}_{ei}\mathbb{H}_i^{n}
\end{array}\right.$$

$$\left\{\begin{array}{lcl}
\mathbf{M}_i^{\varepsilon}\dfrac{\mathbb{E}_i^{n+1}-\mathbb{E}_i^{n}}{\Delta t} & = & \mathbf{G}_i\dfrac{\mathbb{H}_i^{n+1}+\mathbb{H}_i^{n}}{2}-\mathbf{A}_{ie}\mathbb{H}_e^{n+\frac{1}{2}} \\[2ex]
\mathbf{M}_i^{\mu}\dfrac{\mathbb{H}_i^{n}-\mathbb{H}_i^{n+1}}{\Delta t} & = & -{}^{\mathsf{T}}\mathbf{G}_i\dfrac{\mathbb{E}_i^{n}+\mathbb{E}_i^{n+1}}{2}+\mathbf{A}_{ie}\mathbb{E}_e^{n+\frac{1}{2}}
\end{array}\right.$$

$$\left\{\begin{array}{lcl}
\mathbf{M}_e^{\varepsilon}\dfrac{\mathbb{E}_e^{n+1}-\mathbb{E}_e^{n+\frac{1}{2}}}{\Delta t/2} & = & \mathbf{G}_e\mathbb{H}_e^{n+\frac{1}{2}}-\mathbf{A}_{ei}\mathbb{H}_i^{n+1} \\[2ex]
\mathbf{M}_e^{\mu}\dfrac{\mathbb{H}_e^{n+1}-\mathbb{H}_e^{n+\frac{1}{2}}}{\Delta t/2} & = & -{}^{\mathsf{T}}\mathbf{G}_e\mathbb{E}_e^{n+1}+\mathbf{A}_{ei}\mathbb{E}_i^{n+1}
\end{array}\right.$$

Numerical results: 2D case

Scattering of a plane wave by a dielectric cylinder

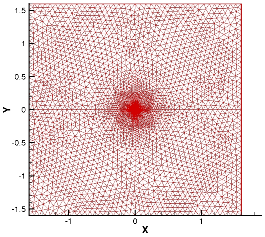

$\#$ vertices = 4,108
$\#$ elements = 8,054

Cylinder: R=0.6 m
F=300 MHz, $\varepsilon_{r,1} = 1.0$ and $\varepsilon_{r,2} = 2.25$

$(\Delta t)_m = 2.09$ picosec
$(\Delta t)_M = 309.63$ picosec

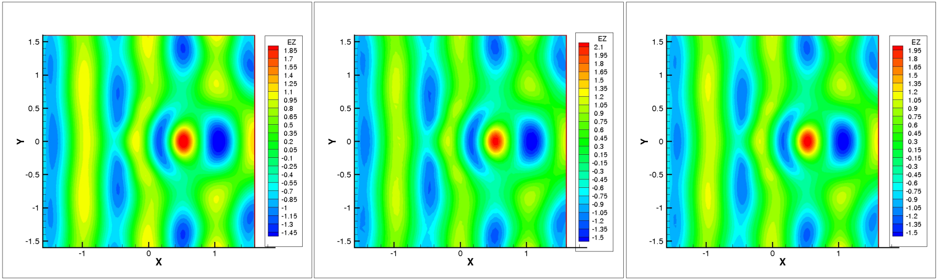

F=300 MHz: contour lines of E_z after 10 periods

Left: exact solution

Middle: implicit DGTD-$\mathbb{P}_1$ method - Right: implicit DGTD-$\mathbb{P}_2$ method

Numerical results: 2D case

Scattering of a plane wave by a dielectric cylinder

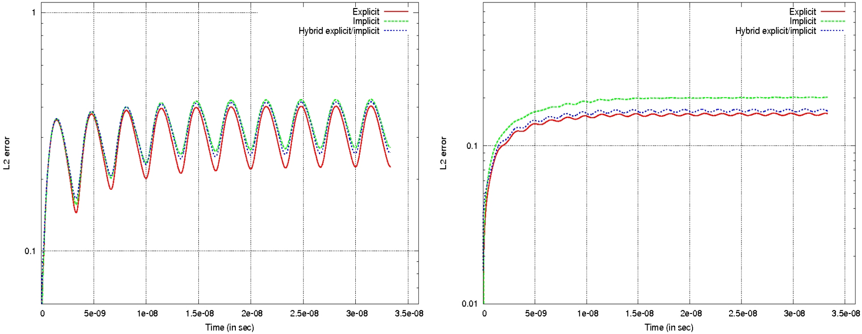

F=300 MHz: time evolution of the L2 error

Left: DGTD-$\mathbb{P}_1$ method - Right: DGTD-$\mathbb{P}_2$ method

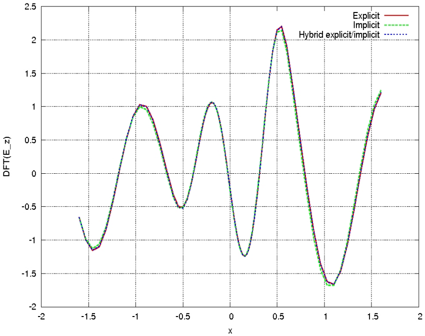

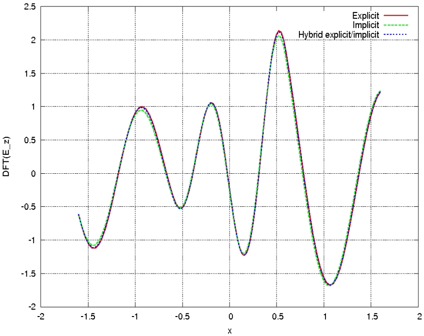

F=300 MHz: 1D distribution of DFT(E_z), $y = 0.0$ m
Left: DGTD-$\mathbb{P}_1$ method - Right: DGTD-$\mathbb{P}_2$ method

- Separation threshold t: triangle area
  - $\min(A_{\tau_i}) = 0.25 \times 10^{-6}$ m^2 and $\max(A_{\tau_i}) = 0.65 \times 10^{-2}$ m^2
  - t $= 10^{-4}$ m^2 $\Rightarrow |\mathcal{S}^e| = 5,745$ and $|\mathcal{S}^i| = 2,309$
  - Reference time step: $\Delta t = 36.575$ picosec

Computing times (AMD Opteron 2 GHz based workstation)

Time integration	Method	CFL-$\mathbb{P}_p$	CPU time	Gain
Explicit	DGTD-$\mathbb{P}_1$	0.3	477 sec	-
Implicit	-	21.0	109 sec	4.4
Hybrid explicit/implicit	-	0.3/17.5	145 sec	3.3
Explicit	DGTD-$\mathbb{P}_2$	0.2	1805 sec	-
Implicit	-	21.0	257 sec	7.0
Hybrid explicit/implicit	-	0.2/17.5	524 sec	3.4

Numerical results: 2D case

Scattering of a plane wave by a dielectric cylinder

- Separation threshold t: triangle area
  - $\min(A_{\tau_i}) = 0.25 \times 10^{-6}$ m^2 and $\max(A_{\tau_i}) = 0.65 \times 10^{-2}$ m^2
  - t $= 10^{-4}$ m^2 $\Rightarrow |\mathcal{S}^e| = 5,745$ and $|\mathcal{S}^i| = 2,309$
  - Reference time step: $\Delta t = 36.575$ picosec

Computing times (AMD Opteron 2 GHz based workstation)
Factorization phase

Time integration	Method	CPU time	Total RAM size
Implicit	DGTD-$\mathbb{P}_1$	3 sec	70 MB
Hybrid explicit/implicit	-	1 sec	18 MB
Implicit	DGTD-$\mathbb{P}_2$	8 sec	181 MB
Hybrid explicit/implicit	-	2 sec	46 MB

- # vertices = 3,815 and # tetrahedra = 19,540
  - $(\Delta t)_m = 0.84$ picosec and $(\Delta t)_M = 107.10$ picosec
  - Separation threshold: specific geometric criterion
  - $|\mathcal{S}^e| = 17,334$ and $|\mathcal{S}^i| = 2,206$
  - Reference time step: $\Delta t = 35.35$ picosec

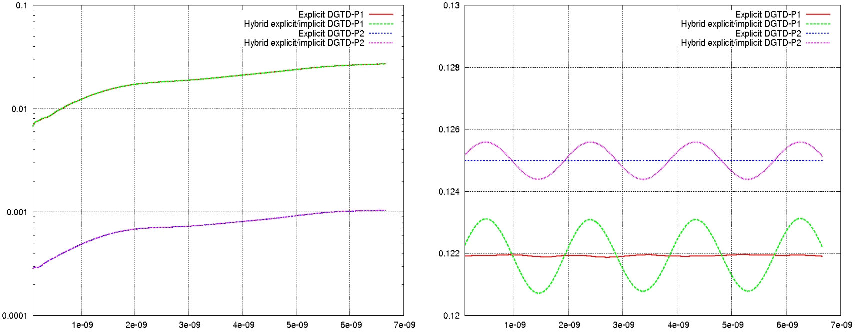

Time evolutions of the L2 error (left) and discrete energy (right)

Numerical results

The 3D case: eigenmode in a metallic cavity

Computing times (Intel Xeon 2.33 GHz based workstation)

Time integration	$\lvert\mathcal{S}^i\rvert$	Method	CFL-$\mathbb{P}_p$	CPU time	Gain
Explicit	-	DGTD-$\mathbb{P}_1$	0.3	2293 sec	-
Hybrid explicit/implicit	2,206	-	0.3/14.0	257 sec	9.0
Explicit	-	DGTD-$\mathbb{P}_2$	0.2	15992 sec	-
Hybrid explicit/implicit	1,259	-	0.2/1.7	5338 sec	3.0
-	1,603	-	0.2/3.3	3561 sec	4.5
-	2,206	-	0.2/7.0	1490 sec	10.7

Factorization phase (Intel Xeon 2.33 GHz based workstation)

Time integration	$\lvert\mathcal{S}^i\rvert$	Method	CPU time	Total RAM size
Hybrid explicit/implicit	2,206	DGTD-$\mathbb{P}_1$	60 sec	341 MB
-	1,259	DGTD-$\mathbb{P}_2$	140 sec	627 MB
-	1,603	-	278 sec	967 MB
-	2,206	-	544 sec	1470 MB

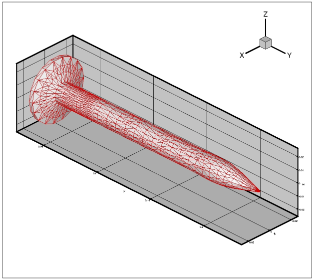

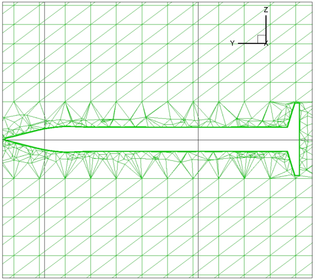

vertices = 71,392 and # elements = 396,312

Scattering of a plane wave by a nail geometry

F=3 GHz, $(\Delta t)_m = 0.25$ picosec, $(\Delta t)_M = 8.43$ picosec

Numerical results

The 3D case: a toy problem

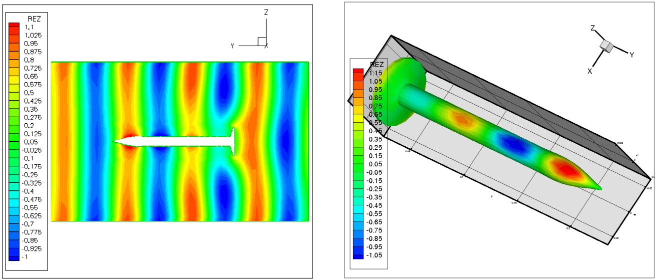

Contour lines of E_z after 5 periods (DGTD-P1 method)
vertices = 71,392 and # elements = 396,312
Scattering of a plane wave by a nail geometry, F=3 GHz

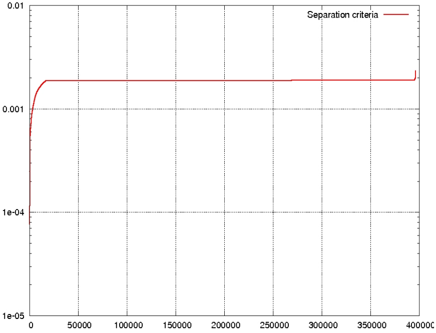

Separation threshold: specific geometric criterion

vertices = 71,392 and # elements = 396,312

Scattering of a plane wave by a nail geometry

F=3 GHz, $(\Delta t)_m = 0.25$ picosec, $(\Delta t)_M = 8.43$ picosec

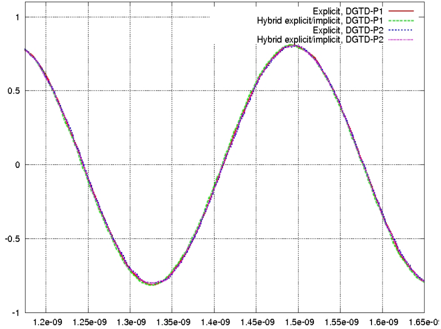

Time evolution of the E_z component at a given point (last of 5 periods)
\# vertices = 71,392 and \# elements = 396,312
Scattering of a plane wave by a nail geometry

- # vertices = 71,392 and # elements = 396,312
  - $(\Delta t)_m = 0.25$ picosec and $(\Delta t)_M = 8.43$ picosec
  - Separation threshold: specific geometric criterion, $t = 10^{-3}$
  - $|\mathcal{S}^e| = 393,256$ and $|\mathcal{S}^i| = 3,056$ (0.8 % of # elements)
  - Reference time step: $\Delta t = 3.33$ picosec

Computing times (Intel Xeon 2.33 GHz based workstation)

Time integration	Method	CFL-$\mathbb{P}_p$	CPU time	Gain
Explicit	DGTD-$\mathbb{P}_1$	0.3	7 h 21 mn	-
Hybrid explicit/implicit	-	0.3/4.3	55 mn	8.0
Explicit	DGTD-$\mathbb{P}_2$	0.2	54 h 26 mn	-
Hybrid explicit/implicit	-	0.2/2.2	6 h 34 mn	8.1

Factorization phase (Intel Xeon 2.33 GHz based workstation)

Time integration	Method	CPU time	Total RAM size
Hybrid explicit/implicit	DGTD-$\mathbb{P}_1$	5 sec	110 MB
-	DGTD-$\mathbb{P}_2$	42 sec	490 MB

Outline

Closure

- Hybrid explicit/implicit (or locally implicit) scheme
  - Well suited to locally refined meshes ($\approx$ 1% of # elements in 3D)
  - Unconditional stability in the refined region (observed in practice)
  - Memory overhead may still be a concern in 3D (if exact LU is used)
- Future works
  - Stability analysis of the hybrid explicit/implicit scheme
  - Parallelization (computational load balancing)
  - Extension to non-conforming locally refined meshes
    - Relying on a DGTD-$\mathbb{P}_{p_i}$ formulation
    - $\mathbb{P}_1$ interpolation in the refined regions (minimal memory overhead)